Multiscale energy spreading in hard-particle chains

Arkady Pikovsky *

Department of Physics and Astronomy, University of Potsdam, Karl-Liebknecht-Str. 24/25, 14476 Potsdam-Golm, Germany

(Received 5 April 2025; accepted 7 July 2025; published 23 July 2025)

We consider a one-dimensional array of particles interacting via an infinite well potential. We explore the properties of energy spreading from an initial state where only a group of particles has nonzero velocities, while others are at rest. We characterize anomalous diffusion of the active domain via moments and entropies of the energy distribution. Only in the special cases of a single-well potential (hard-particle gas) and when the distance between particles is half the potential width, does diffusion exhibit a single scale; otherwise, multiscale anomalous diffusion is observed.

DOI: 10.1103/ddjx-d1dv

I. INTRODUCTION

One-dimensional classical nonlinear lattices possess quite peculiar transport properties. On the one hand, many such systems demonstrate anomalous heat transport, in which the finite-size heat conductivity diverges as a power of the lattice length [1–3]. In a typical setup, one attaches a lattice to two heat baths with different temperatures and measures the energy exchanges with them. Because according to the Green-Kubo theory, conductivity can be expressed in terms of the equilibrium fluctuations of the heat current, anomalous transport manifests itself in a nonintegrable power-law decay of the correlation function of the energy current [4]. Another manifestation of anomalous heat transport is a superdiffusive spreading of local energy perturbations on top of the equilibrium state with finite temperature (finite energy density) [5]. Theoretical and numerical findings about anomalous heat transport have been confirmed in experiments [6–9].

Another setup where one-dimensional lattices demonstrate nontrivial transport properties is the spreading of initially localized perturbations on top of a zero-temperature state. Due to the effect of Anderson localization [10], in a linear lattice, even a small amount of disorder leads to exponential localization of eigenmodes, which blocks spreading at large times. However, the nonlinearity of the lattice may result in chaos, which destroys localization and leads to subdiffusive spreading. One popular example is a disordered nonlinear Schroedinger lattice [11–14]. However, even for this widely studied model, it is still not clear whether spreading persists at very large times, as chaos may degenerate into localized quasiperiodic modes [15,16]. Spreading in a nonlinear Schroedinger lattice has been observed in optical experiments [17]. While in the context of the Schroedinger lattice, one follows the spreading of the wave packet, for nonlinear lattices of Klein-Gordon or Fermi-Pasta-Ulam-Tsingoi type, one studies the spreading of energy from a localized perturbation on top of a zero-temperature state [18–22]. While in many numerical experiments a subdiffusive spreading is observed, asymptotic regimes at large times remain elusive. For the experimental realization of such a spreading in a disordered granular chain, see Ref. [23].

In this paper, we explore energy spreading on top of a zero-temperature state for hard-particle models previously studied in the context of anomalous heat transport. These models share basic properties, such as conservation of momentum, with lattices possessing smooth coupling potentials, but allow for an efficient numerical implementation. We will demonstrate that, while in some cases anomalous superdiffusion or subdiffusion, characterized by a single exponent (monoscale diffusion), is observed, a hard-particle chain generally exhibits multiscaled diffusion, where differently defined "lengths" of the spreading domain grow with different exponents.

II. MODEL FORMULATION

Our basic model is a one-dimensional chain of particles interacting via an infinite well potential [24–26]. This hard-particle chain (HPC) is defined via the Hamilton function

$$H = \sum_i \frac{p_i^2}{2m_i} + U(x_{i+1} - x_i),$$
$$U(\Delta x) = \begin{cases} \infty & \Delta x < 0 \text{ and } \Delta x > a^{-1}, \\ 0 & 0 \leqslant \Delta x \leqslant a^{-1}. \end{cases} \quad (1)$$

The essential dimensionless parameter of the problem is $0 \leqslant a < 1$, the ratio of the mean distance between the particles and the potential width. We set the initial distance between the particles to 1; thus, the parameter a enters the definition of the potential (the width of the well) in (1). To ensure the

*Contact author: pikovsky@uni-potsdam.de

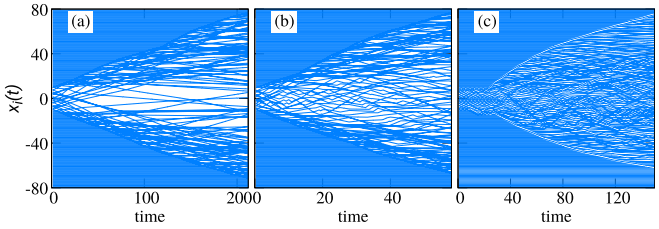

FIG. 1. Examples of the energy spreading process: trajectories $x_i(t)$ of particles vs time for three values of parameter a: panel (a) $a = 0$; panel (b) $a = 0.25$; panel (c) $a = 0.5$.

dynamics is nonintegrable, we set random masses according to a uniform distribution $0.5 \leqslant m_i \leqslant 1.5$.

In the case $a = 0$, the double-well potential becomes a hard-core potential, and the model reduces to a famous one-dimensional hard-particle gas (HPG) model [27–29], where only elastic collisions at $x_{i+1} = x_i$ happen. Remarkably, the HPC model is symmetric with respect to the change of the parameter $a \to 1 - a$ [26]. The value $a = 1/2$ is special because here, the two types of collisions at $x_{i+1} = x_i$ and at $x_{i+1} = x_i + a^{-1}$ become equally probable in equilibrium, and the pressure vanishes. Therefore, we restrict our attention below to the interval $0 \leqslant a \leqslant 1/2$.

The HPC (1) conserves energy and momentum, and in the heat transfer setup has demonstrated anomalous heat conductivity [24–26]. Below in this paper, we study energy-spreading properties at zero temperature. We start with a configuration where positions are equidistant $x_i(0) = i$, and the momenta p_i of the particles are randomly set in a small domain (ten sites) around $i = 0$, other particles are at rest $p_i(0) = 0$. Due to the possibility of time rescaling, without loss of generality, the total energy can be set to unity. Furthermore, we set the total initial momentum to zero.

III. ENERGY SPREADING AND ITS CHARACTERIZATION

In numerical simulations, we followed the straightforward approach described in [24,28]. After each collision, we know the positions and velocities of all particles, and can explicitly express, by solving equations of the free motion of particles, the time intervals to all possible future collisions according to conditions $x_{i+1} = x_i$, $x_{i+1} = x_i + a^{-1}$. Finding the minimum over these intervals allows us to calculate all trajectories and find all positions and velocities just prior to the next collision. After that, we apply simple expressions from Ref. [24] to express the velocities of colliding particles after the collision through their velocities before the collision. We also note that statistical fluctuations due to initial conditions and random particle masses are negligible, so that additional averaging over samples of these random parameters was not necessary.

The phenomenology of the dynamics is simple (Fig. 1): more and more particles are involved in the nontrivial dynamics via collisions, and a spreading "active domain" consisting of particles having nonzero energy is formed. At each time instant, only a finite number of particles belong to the active domain, and this number $L(t)$ is a natural measure of the domain width. However, this number is only one of the possible definitions of the domain width. Because we normalize the total energy to one, and the energies of the

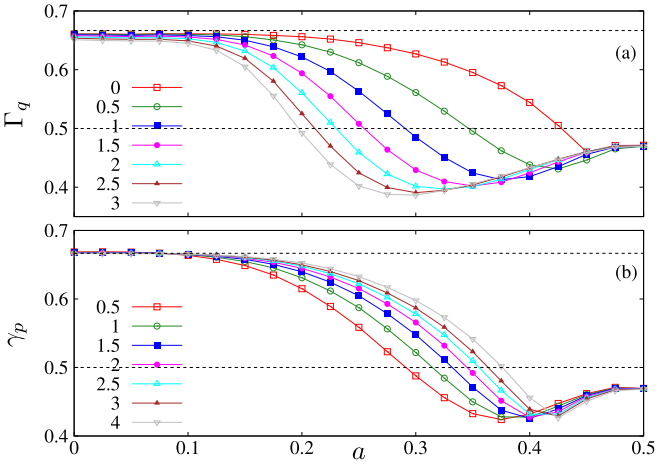

FIG. 2. Power law growth rates in dependence on the indices and parameter a. Panel (a): exponents Γ_q for indices q indicated in the marker descriptions; panel (b): exponents γ_p for indices p indicated in the marker descriptions. The dotted black lines show values $2/3$ and $1/2$.

particles are non-negative, the set of local energies $E_i = p_i^2/(2m_i)$ can be interpreted as a probability distribution. Accordingly, we can characterize the distribution width using the moments or entropies of this distribution.

In the former approach, we define the "center of energy" $\langle x \rangle$, the moments M_p, and the corresponding moment-based sizes of the domain ℓ_p according to relations

$$\langle x \rangle = \sum_i x_i E_i, \quad M_p = \sum_i |x_i - \langle x \rangle|^p E_i, \quad \ell_p = (M_p)^{1/p}. \quad (2)$$

Here, the indices $p > 0$ need not be integers.

Another way to characterize distributions is to calculate their Renyi entropies I_q depending on the index $q \geqslant 0$, and to use them to define the widths $\mathcal{L}_q$:

$$I_q = \frac{\log \sum_i E_i^q}{1 - q}, \quad \mathcal{L}_q = \exp[I_q]. \quad (3)$$

Note that for $q = 0$, the entropy is the logarithm of the support of the distribution $I_0 = \log L$, thus $L = \mathcal{L}_0$. Another widely used case is $q = 2$, which corresponds to the participation number, a concept commonly applied in the context of wave packet spreading.

Plots of the lengths ℓ_p, $\mathcal{L}_q$ reveal that these quantities grow as power laws: $\ell_p \sim t^{\gamma_p}$, $\mathcal{L}_q \sim t^{\Gamma_q}$ (cf. observation of index-dependent growth powers of the moments for dynamically generated diffusion processes in Refs. [30,31]). We present these powers as functions of the parameter a in Fig. 2.

The main conclusion from the data of Fig. 2 is that the powers for all the indices coincide if $a = 0$ (pure HPG) or $a = 1/2$ (HPC with zero pressure in equilibrium), so that one can speak of monoscale spreading in these cases. In contradistinction, in between, there is a strong dependence of exponents γ_p, Γ_q on indices p, q, manifesting multiscale spreading (in the context of diffusion processes, one speaks in this case of "strong anomalous diffusion" [32]). We illustrate these dependencies in a larger range of indices for $a = 1/4$ in Fig. 3.

We stress that in all cases, the diffusive spreading of the energy is nontrivial: it is superdiffusive for small a and

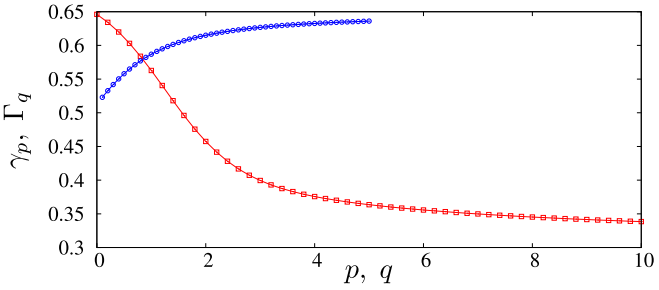

FIG. 3. Power law exponents in dependence of indices for $a = 0.25$. Red squares: entropies-based exponents Γ_q; blue circles: moments-based exponents γ_p.

subdiffusive for a close to $1/2$. However, for $0.2 \lesssim a \lesssim 0.4$, some exponents are larger than $1/2$ and some smaller than $1/2$, as illustrated in Fig. 3. In particular, for $a = 0$ (HPG case), one observes $\gamma_p \approx \Gamma_q \approx 2/3$. This power can be obtained from the following simple scaling arguments. Suppose that the energy is nearly uniformly distributed among L active particles. Then, the energy of the boundary particle is $\sim L^{-1}$, and its velocity is $\sim L^{-1/2}$. The time to hit the next resting particle outside the active domain is inversely proportional to the velocity, and after this happens, the active domain increases by 1. Thus, $dt/dL \sim L^{1/2}$ and solving this equation we get $t \sim L^{3/2}$. This yields the scaling law for the domain spreading $L \sim t^{2/3}$. The same scaling has been observed in [33] for a similar setup with nonrandom, but alternating masses of the particles; in this paper, connections of the problem to the hydrodynamic Euler equations are also discussed (cf. [34]).

IV. SCALING PROPERTIES OF THE DISTRIBUTIONS

Next, we describe the scaling properties of the distributions of the active particles. We introduce the coarse-grained density of the particles and two coarse-grained distributions of energy: the energy per particle distribution and the energy density. To scale these distributions, we note that $L(t)$ represents the length of the active domain and the number of active particles, as the spacing in our setup is 1. So we introduce the normalized particle index $\nu = (i - i_{\text{left}})L^{-1}$, $0 \leqslant \nu \leqslant 1$, and the normalized particle position $\xi = (x_i - x_{i_{\text{left}}})L^{-1} - 0.5$, $-0.5 \leqslant \xi \leqslant 0.5$. Here, i_{left} is the index of the left-most active particle (left border of the active domain). Thus, plotting i vs x_i we obtain a cumulative distribution of particles in scaling coordinates $\nu(\xi)$, and its derivative yields the particle density $\rho(\xi) = \frac{d\nu}{d\xi}$. Similarly, we introduce the cumulative energy as $\epsilon_i = \sum_{k=i_{\text{left}}}^{i} E_k$, so that $0 \leqslant \epsilon \leqslant 1$. By plotting ϵ_i vs i we obtain a curve $\epsilon(\nu)$ which yields the density of energy per particle $W(\nu) = \frac{d\epsilon}{d\nu}$. The density of energy $w(\xi) = \frac{d\epsilon}{d\xi}$ can be obtained from the obvious relation $w(\xi) = W(\nu)\rho(\xi)$.

To distinguish monoscale and multiscale regimes, we must compare densities occurring at different sizes L of the active domain. If these densities coincide, then the length L delivers a complete characterization of the distributions, and all the powers γ_p, Γ_q are equal. Multiscaling occurs if the densities at different values of length L have different shapes.

The first observation from the numerics is that the renormalized particle density $\rho(\xi)$ does not depend on length L,

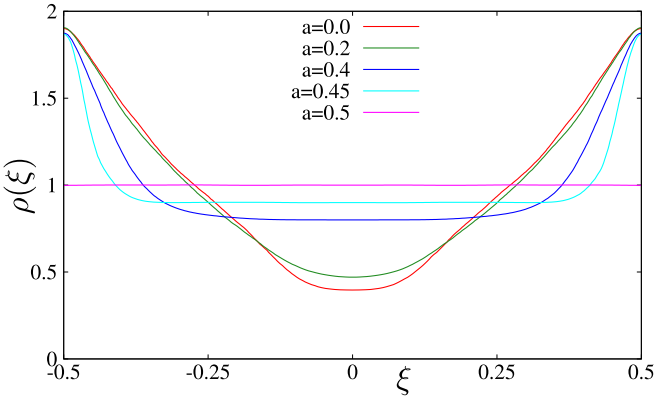

FIG. 4. Densities $\rho(\xi)$ for different values of parameter a.

for sufficiently large L. The profiles at different parameter values a are shown in Fig. 4. Notice that the density outside the active domain is $\rho = 1$. For a close to zero, two steps of size ≈ 0.8 are formed at the borders of the active domain, and these "shocks" propagate superdiffusively. For larger a, the distribution in the bulk becomes nearly flat, and the dense shock regions become thinner. Finally, at $a = 0.5$, the shocks disappear, and the density over the active domain is uniform $\rho = 1$.

Next, we discuss the energy distributions $W(\nu)$ and $w(\xi)$. In Fig. 5, we show the coarse-grained energy-per-particle distribution densities at several values of parameter a at two different instants of time: one at which the total width of the active domain is $L = 10^4$ and another one at which $L = 4 \cdot 10^4$. One can see that for $a = 0$, these densities practically coincide, while for other values of a, they are significantly different. This corresponds well with multiscaling at these values of a. The energy-per-particle distributions possess a "hot core" of locally highly energetic particles at the center of the active domain. This is accompanied by tails of particles with relatively low energy; in these tails, however, energy grows toward the edges of the active domain.

At the value of parameter $a = 1/2$, the monoscaling property is restored, and the spatial densities of energy $W(\xi)$ presented in Fig. 6 at two sizes of the active domain practically coincide. We note that here the profiles $W(\nu)$ and $w(\xi)$ are the same because the density $\rho(\xi)$ is constant (cf. Fig. 4). We

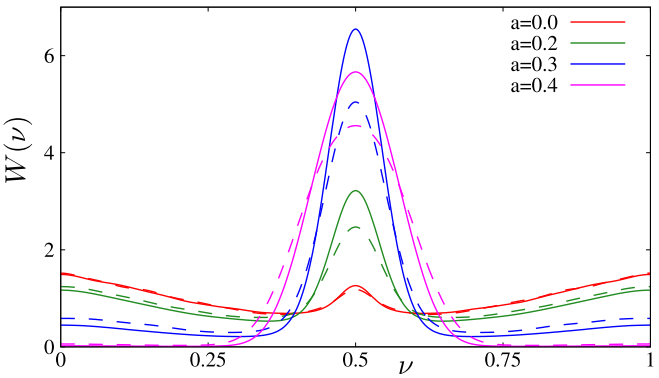

FIG. 5. Densities of energy per particle $W(\nu)$ for different values of parameter a. Full lines at $L = 4 \cdot 10^4$, dashed lines at $L = 10^4$.

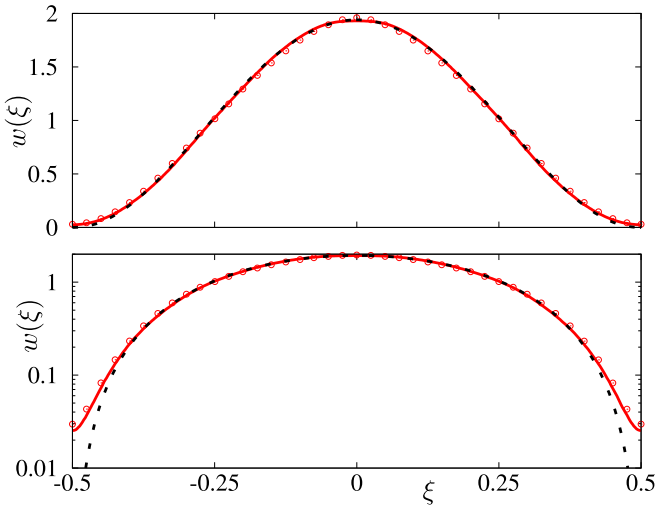

FIG. 6. Density of energy $w(\xi)$ for $a = 1/2$, in the linear and in the logarithmic formats. Full lines at $L = 4 \cdot 10^4$, red circles at $L = 2 \cdot 10^4$. Black dashed line is the fit discussed in the text.

discuss the profile at $a = 1/2$ in more detail because of its simple one-hump form. The spreading of energy at $a = 1/2$ is subdiffusive, with the exponent ≈0.47 (see Fig. 2). This allows a tempting attempt at a simple phenomenological model for such a spreading. Indeed, the nonlinear diffusion equation,

$$\partial_t u(x,t) = \partial_{xx} u^{c+1}, \quad c > 0, \tag{4}$$

describes a subdiffusive spreading of the quantity u, the integral of which is conserved. The self-similar solution has the scaling form $u \sim t^{-\beta}(1 - 4(x/L(t))^2)^{\alpha}$. This solution has finite support $|x| \leqslant L/2$ with $L(t) \sim t^{\beta}$, where the power $\beta < 1/2$ is the single exponent of the subdiffusive spreading. The exponents α, β are determined by the nonlinearity parameter c: $\beta = 1/(c+2)$, $\alpha = 1/c$. Remarkably, the shape of the energy density profile observed numerically at $a = 1/2$ is very well fitted by the form predicted by the solution of the nonlinear diffusion equation [see the black dashed curve in Fig. 6 which is the function $w_{fit}(\xi) = A(1 - 4\xi^2)^B$ with $A \approx 1.94$ and $B \approx 2.2$]. The powers, however, do not satisfy the relation $\alpha^{-1} = \beta^{-1} - 2$ predicted by the nonlinear diffusion equation. Indeed, the observed value for the spreading exponent $\beta = 0.47$ corresponds to $c \approx 0.128$, but for this value of c, the power of the profile shape of Eq. (4) should be $\alpha \approx 7.8$, which is very far from the fitted value 2.2.

V. DISCUSSION

Here, we compare the properties of the HPC and the HPG models with other cases, where multiscaling anomalous spreading has been observed. A typical situation of multiscaling in anomalous diffusion, explored in Refs. [31,32], is that of a combination of a diffusive process with ballistic modes. The latter modes describe the spreading of the support of the distribution with constant speed, so that the moment-based exponent tends to 1 for high-order moments: $\gamma_p \to 1$ as $p \to \infty$. Furthermore, typical for such situations is a piecewise-linear shape of the dependence $p\gamma_p$ on p [31,32]. This type of energy spreading has been observed in Refs. [24,35,36]. However, in these studies, one considered the spreading of an energy hump on top of an equilibrium state with finite energy density. Correspondingly, the ballistic mode can be associated with sound waves [24]. In contradistinction, in our case of spreading of energy on top of zero-temperature equilibrium, the leading "modes" defining propagation of the active domain are not ballistic but super- or subdiffusive. Correspondingly, the shape of the dependence of $p\gamma_p$ on p is a smooth curve (Fig. 3) rather than a piecewise-linear line conjectured in [32]. One possible theoretical approach to explaining multiscaling could be considering separately the core and the tails of the energy density presented in Fig. 5, similar to what has been done for the HPG case in [33].

VI. CONCLUSIONS

In summary, we have demonstrated multiscaled energy spreading from a local in space disturbance in the simple model of a hard-particle chain (1). Different effective lengths of the spreading domain, defined via moments of different orders or different Rényi entropies of the distribution of energies, depend on time via power laws with different, index-dependent exponents. Correspondingly, the shapes of the energy distributions at different times are not self-similar but show a clear separation in the central peak and tails, obeying different scalings. Contrary to previous cases where ballistically spreading tails have been reported, here, the tails spread superdiffusively.

In two remarkable limits, monoscaling is observed, with a self-similar behavior of the energy profile. For a hard-particle gas, which corresponds to a single-well coupling potential, we observe superdiffusive spreading with exponent ≈2/3 following simple scaling arguments. Here, however, the profile is nontrivial: the particle density has a minimum at the center of the domain and maxima at the edges, thus building superdiffusively spreading shocks. The energy per particle density exhibits a weak maximum in the middle of the domain, and at the borders, the energy density also reaches its maximum.

Another special case is a symmetric hard-particle chain with the mean distance between the particles being exactly half the potential's width. Here, in equilibrium, the pressure of the gas vanishes. We observe here a constant density of the subdiffusively (exponent ≈0.47) spreading domain. The distribution of energies is a one-hump profile that very much resembles a profile of a self-similar solution to a nonlinear diffusion equation. However, the profile shape and the spreading exponent do not follow the relation predicted by the solution to the diffusion equation.

An intriguing question is whether the multiscaling observed can also occur in smooth or continuous potentials. For example, in the hard-particle gas limit $a = 0$, one can replace hard particles with a more realistic model of colliding elastic spheres, interacting via Hertz law [20,21,23]. Another extension of the present study could be the consideration of momentum-conserving variants of the ding-a-ling model [37,38] which combine hard-wall and continuous interaction potentials.

ACKNOWLEDGMENT

I thank Ph. Rosenau, A. Politi, and H. Chaté for useful discussions.

DATA AVAILABILITY

All the data are created using standard numerical approaches are available within the article. All the data are created using standard numerical approaches are not publicly available upon publication because it is not technically feasible and/or the cost of preparing, depositing, and hosting the data would be prohibitive within the terms of this research project. The data are available from the authors upon reasonable request.

[1] *Thermal Transport in Low Dimensions. From Statistical Physics to Nanoscale Heat Transfer*, edited by S. Lepri, Lecture Notes in Physics Vol. 921 (Springer, Heidelberg, 2016).

[2] R. Livi, Anomalous transport in low-dimensional systems: A pedagogical overview, Physica A **631**, 127779 (2023).

[3] G. Benenti, D. Donadio, S. Lepri, and R. Livi, Non-Fourier heat transport in nanosystems, La Rivista del Nuovo Cimento **46**, 105 (2023).

[4] S. Lepri, R. Livi, and A. Politi, On the anomalous thermal conductivity of one-dimensional lattices, Europhys. Lett. **43**, 271 (1998).

[5] P. Cipriani, S. Denisov, and A. Politi, From anomalous energy diffusion to Lévy walks and heat conductivity in one-dimensional systems, Phys. Rev. Lett. **94**, 244301 (2005).

[6] C. W. Chang, D. Okawa, H. Garcia, A. Majumdar, and A. Zettl, Breakdown of Fourier's law in nanotube thermal conductors, Phys. Rev. Lett. **101**, 075903 (2008).

[7] M. Upadhyaya and Z. Aksamija, Nondiffusive lattice thermal transport in Si-Ge alloy nanowires, Phys. Rev. B **94**, 174303 (2016).

[8] A. Crnjar, C. Melis, and L. Colombo, Assessing the anomalous superdiffusive heat transport in a single one-dimensional pedot chain, Phys. Rev. Mater. **2**, 015603 (2018).

[9] L. Yang, Y. Tao, Y. Zhu, M. Akter, K. Wang, Z. Pan, Y. Zhao, Q. Zhang, Y.-Q. Xu, R. Chen *et al.*, Observation of superdiffusive phonon transport in aligned atomic chains, Nat. Nanotechnol. **16**, 764 (2021).

[10] *50 Years Of Anderson Localization*, edited by P. W. Anderson (World Scientific, Singapore, 2010).

[11] A. S. Pikovsky and D. L. Shepelyansky, Destruction of Anderson localization by a weak nonlinearity, Phys. Rev. Lett. **100**, 094101 (2008).

[12] S. Flach, D. O. Krimer, and C. Skokos, Universal spreading of wave packets in disordered nonlinear systems, Phys. Rev. Lett. **102**, 024101 (2009).

[13] S. Fishman, Y. Krivolapov, and A. Soffer, The nonlinear Schrödinger equation with a random potential: Results and puzzles, Nonlinearity **25**, R53 (2012).

[14] S. Flach, Nonlinear lattice waves in random potentials, in *Nonlinear Optical and Atomic Systems: At the Interface of Physics and Mathematics*, edited by C. Besse and J.-C. Garreau, Lecture Notes in Mathematics Vol. 2146 (Springer, Cham, 2015), pp. 1–48.

[15] A. Pikovsky and S. Fishman, Scaling properties of weak chaos in nonlinear disordered lattices, Phys. Rev. E **83**, 025201(R) (2011).

[16] S. Aubry, Diffusion without spreading of a wave packet in nonlinear random models, in *Chaos, Fractals and Complexity*, edited by T. Bountis, A. Provata, Y. Komminis, F. Vallianatos, and D. Kugiumtzis, Springer Proceedings in Complexity (Springer, Cham, 2023), pp. 3–36.

[17] Y. Lahini, R. Pugatch, F. Pozzi, M. Sorel, R. Morandotti, N. Davidson, and Y. Silberberg, Observation of a localization transition in quasiperiodic photonic lattices, Phys. Rev. Lett. **103**, 013901 (2009).

[18] M. Mulansky, K. Ahnert, and A. Pikovsky, Scaling of energy spreading in strongly nonlinear disordered lattices, Phys. Rev. E **83**, 026205 (2011).

[19] M. Mulansky and A. Pikovsky, Energy spreading in strongly nonlinear disordered lattices, New J. Phys. **15**, 053015 (2013).

[20] A. J. Martínez, P. G. Kevrekidis, and M. A. Porter, Superdiffusive transport and energy localization in disordered granular crystals, Phys. Rev. E **93**, 022902 (2016).

[21] A. Ngapasare, G. Theocharis, O. Richoux, C. Skokos, and V. Achilleos, Chaos and anderson localization in disordered classical chains: Hertzian versus Fermi-Pasta-Ulam-Tsingou models, Phys. Rev. E **99**, 032211 (2019).

[22] A. Pikovsky, Scaling of energy spreading in a disordered Ding-Dong lattice, J. Stat. Mech. (2020) 053301.

[23] E. Kim, A. J. Martínez, S. E. Phenisee, P. Kevrekidis, M. A. Porter, and J. Yang, Direct measurement of superdiffusive energy transport in disordered granular chains, Nat. Commun. **9**, 640 (2018).

[24] L. Delfini, S. Denisov, S. Lepri, R. Livi, P. K. Mohanty, and A. Politi, Energy diffusion in hard-point systems, Eur. Phys. J.: Spec. Top. **146**, 21 (2007).

[25] A. Politi, Heat conduction of the hard point chain at zero pressure, J. Stat. Mech. (2011) P03028.

[26] C. Mejía-Monasterio, A. Politi, and L. Rondoni, Heat flux in one-dimensional systems, Phys. Rev. E **100**, 032139 (2019).

[27] G. Casati, Energy transport and the Fourier heat law in classical systems, Found. Phys. **16**, 51 (1986).

[28] P. Grassberger, W. Nadler, and L. Yang, Heat conduction and entropy production in a one-dimensional hard-particle gas, Phys. Rev. Lett. **89**, 180601 (2002).

[29] S. Lepri, R. Livi, and A. Politi, Too close to integrable: Crossover from normal to anomalous heat diffusion, Phys. Rev. Lett. **125**, 040604 (2020).

[30] I. Aranson, M. Rabinovich, and L. S. Tsimring, Anomalous diffusion of particles in regular fields, Phys. Lett. A **151**, 523 (1990).

[31] A. S. Pikovsky, Statistical properties of dynamically generated anomalous diffusion, Phys. Rev. A **43**, 3146 (1991).

[32] P. Castiglione, A. Mazzino, P. Muratore-Ginanneschi, and A. Vulpiani, On strong anomalous diffusion, Physica D **134**, 75 (1999).

[33] S. Chakraborti, S. Ganapa, P. L. Krapivsky, and A. Dhar, Blast in a one-dimensional cold gas: From newtonian dynamics to hydrodynamics, Phys. Rev. Lett. **126**, 244503 (2021).

[34] P. I. Hurtado, Breakdown of hydrodynamics in a simple one-dimensional fluid, Phys. Rev. Lett. **96**, 010601 (2006).

[35] F. Piazza and S. Lepri, Heat wave propagation in a nonlinear chain, Phys. Rev. B **79**, 094306 (2009).

[36] S. Lepri, R. Schilling, and S. Aubry, Asymptotic energy profile of a wave packet in disordered chains, Phys. Rev. E **82**, 056602 (2010).

[37] G. R. Lee-Dadswell, E. Turner, J. Ettinger, and M. Moy, Momentum conserving one-dimensional system with a finite thermal conductivity, Phys. Rev. E **82**, 061118 (2010).

[38] Z. Gao, N. Li, and B. Li, Heat conduction and energy diffusion in momentum-conserving one-dimensional full-lattice ding-a-ling model, Phys. Rev. E **93**, 022102 (2016).